Journal of Power Sources 245 (2014) 283–291

Contents lists available at SciVerse ScienceDirect

Journal of Power Sources

journal homepage: www.elsevier.com/locate/jpowsour

Effect of poly(ethylene oxide) on ionic conductivity and electrochemical properties of poly(vinylidenefluoride) based polymer gel electrolytes prepared by electrospinning for lithium ion batteries

Raghavan Prasanth [a,b], Nageswaran Shubha [a], Huey Hoon Hng [a], Madhavi Srinivasan [a,b,*]

[a] School of Materials Science and Engineering, Nanyang Technological University, Block N4.1, 50 Nanyang Avenue, Singapore 639798, Singapore
[b] Energy Research Institute @ NTU (ERI@N) Research Techno Plaza, 50 Nanyang Drive, Singapore 637553, Singapore

HIGHLIGHTS

- Effect of PEO on electrochemical properties of electrospun PVdF based PEs studied.
- PEs are prepared by activating membrane with lithium salts in carbonate solvents.
- PEs show high ionic conductivity and good compatibility with lithium electrodes.
- Li/$LiFePO_4$ cell using PVdF/PEO delivers significantly higher discharge capacity.
- The cells show stable cycle performance under continuous cycling.

GRAPHICAL ABSTRACT

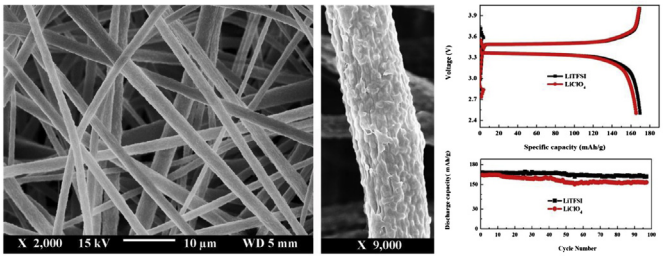

ARTICLE INFO

Article history:
Received 27 March 2013
Received in revised form
21 May 2013
Accepted 21 May 2013
Available online 21 June 2013

Keywords:
Polymer electrolyte
Lithium ion batteries
Polymer blend
Electrospinning
Fibrous membrane

ABSTRACT

Effect of poly(ethylene oxide) on the electrochemical properties of polymer electrolyte based on electrospun, non-woven membrane of PVdF is demonstrated. Electrospinning process parameters are controlled to get a fibrous membrane consisting of bead-free, uniformly dispersed thin fibers with diameter in the range of 1.5–1.9 μm. The membrane with good mechanical strength and porosity exhibits high uptake when activated with the liquid electrolyte of lithium salt in a mixture of organic solvents. The polymer gel electrolyte shows ionic conductivity of 4.9×10^{-3} S cm^{-1} at room temperature. Electrochemical performance of the polymer gel electrolyte is evaluated in Li/polymer electrolyte/$LiFePO_4$ coin cell. Good performance with low capacity fading on charge–discharge cycling is demonstrated.

1. Introduction

Polymer electrolytes (PEs) have received considerable attention in recent years for application in lithium ion batteries [1–5]. Poly(ethylene oxide) (PEO)-based electrolyte has been widely studied as solid polymer electrolyte due to its good thermal properties, mechanical properties and interfacial stability with lithium metal. It has ether linkages, with oxygen atoms present at a suitable inter-atomic

* Corresponding author. School of Materials Science and Engineering, Nanyang Technological University, Block N4.1, 50 Nanyang Avenue, Singapore 639798, Singapore. Tel.: +65 67904606; fax: +65 67909081.
E-mail address: madhavi@ntu.edu.sg (M. Srinivasan).

0378-7753/$ – see front matter © 2013 Elsevier B.V. All rights reserved.
http://dx.doi.org/10.1016/j.jpowsour.2013.05.178

separation to allow segmental motion of the polymeric chain which is beneficial for facile ionic conduction [2]. The prototypical solid PE is PEO-LiX, prepared by blending PEO with lithium salt (LiX) of a large anion [6,7]. The transport of Li^+ ions in these electrolytes has been associated with the local relaxation and segmental motion of the amorphous regions in the PEO chains. Due to the formation of crystallites in PEO systems, these polymers often show high crystallinity and low ionic conductivity (typically $\leq 10^{-5}$ S cm^{-1}) at low temperatures. This necessitates operation at higher temperatures (generally, >70 °C) for their successful utilization in practical battery applications. The most straightforward approach to overcome this problem is to modify the solvating polymer in order to decrease the crystallinity and glass transition temperature of the PE, while retaining the excellent solvating properties of the ethylene oxide chain. Efforts have been made to provide such an environment for increasing the ionic conductivity at low temperatures. Several approaches have been examined, including use of copolymers, blending with other polymers, addition of plasticizers and cross-linking [8]. PEO is soluble in common battery electrolytes like ethylene carbonate (EC) and diethyl carbonate (DEC), which limits its use in dimensionally stable PGEs, so PEO is mostly studied as solid polymer electrolyte. Therefore, the present study aims to develop polymer gel electrolyte (PGE) which utilizes the advantageous electrochemical properties of PEO. For that, PVdF is blended with PEO, and the effect of PEO on ionic conductivity and electrochemical properties of PVdF based PGEs is studied. The presence of PVdF in the polymer blend retains the mechanical properties of the membrane, while the ether linkages with oxygen atoms in PEO help to improve the segmental motion and dissociation of lithium salts.

PVdF is specifically selected to prepare polymer blend with PEO due to its compatibility with PEO, excellent electrochemical stability and affinity to liquid electrolyte. PVdF has a strong electron withdrawing fluorine atom in its back bone and high dielectric constant ($\varepsilon \approx 8.4$). Thus, the polymer blend effectively dissociates lithium salts to generate a large quantity of charge carriers for conduction [9,10]. In the present study, PGEs have been prepared by immobilizing the porous polymeric film prepared by electrospinning with liquid electrolyte. The electrospun membranes appear to be particularly suitable as host matrices in microporous polymer gel electrolytes, because the fully interconnected pores have large surface area that can function as efficient channels for ion conduction [11].

The nature of the liquid electrolyte used to activate the polymer to form PGE affects the properties of the PGE significantly. Different lithium salts have different electrochemical properties which affect ion dissociation, ion diffusion, ion transference number, electrochemical stability etc [1,12,13]. Also they interact differently with polymeric matrices affecting the ionic coupling [13]. In this work, five different lithium salts have been studied to understand their compatibility with the electrospun PVdF/PEO polymer membrane as battery electrolyte cum separator and their electrochemical properties studied to choose the best performing electrolyte for this polymeric system. The suitability of the PGEs based on electrospun PVdF/PEO polymer blend membrane for room temperature lithium metal polymer batteries is also investigated.

2. Experimental

2.1. Preparation of PVdF/PEO blend membrane

PVdF (M*w*, 53,4000, Sigma Aldrich) and PEO (M*v*, 100,000 Sigma Aldrich), were vacuum dried at 60 °C for 6 h before use. Solvents, acetone and *N*,*N*-dimethyl acetamide (DMAc) (HPLC grade, Aldrich) were used as received. Uniform solution of 90% PVdF and 10% PEO in a mixed solvent of acetone/DMAc (7:3, w/w) was prepared by magnetic stirring for 24 h at room temperature. Polymer/solvent (w/w) ratios for all the final solutions were kept at 16 wt.% solid content. The resulting solution was kept for 15 min to get bubble free clear solution in air tight container. Sufficient quantity of the solution was fed to the steel needle using a syringe infusion/withdrawal pump (KD Scientific, Model-210). The tip of the needle was connected to high voltage source and electrospun at ambient atmosphere. The essential electrospinning parameters were as follows: applied voltage 18–20 kV (depends on the viscosity of the solution), working distance from collector to tip of the spinneret ~20 cm, bore size of the needle 0.6 mm, solution feed rate 0.2 ml min^{-1} and collector drum rotation speed 150 rpm. The as spun fibers in the form of free standing nonwoven membrane of average thickness ~150 μm with sufficient mechanical strength was collected on a grounded, aluminum drum wrapped with a thin aluminum foil. Further, the membrane was dried at room temperature on the drum for 6 h to prevent the shrinking of fibers and then removed from the collection drum. Final drying of the membrane was carried out in a vacuum oven at 60 °C for 12 h to remove any traces of solvent. The dried membrane was transferred to a dry box at 25 °C (H_2O level < 20 ppm) for further use.

2.2. Preparation of electrolytes

1 M $LiPF_6$ in EC/DEC (1:1, w/w) (Danvec on Technologies Pvt. Ltd), EC and DEC (Sigma Aldrich) was used as received. LiTFSI, $LiCF_3SO_3$, $LiClO_4$, and $LiBF_4$ (Sigma Aldrich) were vacuum dried and transferred to argon-filled glove box with oxygen and moisture level <0.1 ppm. The electrolytes were prepared by dissolving required amount of lithium salts in EC/DEC (1:1 w/w) to get 1 M solution.

2.3. Characterization of PVdF/PEO blend membranes

Surface morphology of membranes were examined with high resolution field-emission scanning electron microscope (FE-SEM: JEOL JSM7600F) at an accelerating voltage of 15 kV. The samples were mounted on metal stubs using conductive double-sided carbon tape, and a thin layer of platinum was sputtered on the sample using JEOL JFC-1200 prior to scanning. Average fiber diameter (AFD) (~300 fibers) was estimated from the micrograph taken at high magnification. Porosity (*P*) was determined by immersing the dry membrane in *n*-butanol for 1 h. Following relation was used to calculate the porosity:

$$P(\%) = \frac{M_{\mathrm{BuOH}}/\rho_{\mathrm{BuOH}}}{M_{\mathrm{BuOH}}/\rho_{\mathrm{BuOH}} + M_m/\rho_P} \times 100$$

where M_m is the mass of the dry membrane, M_{BuOH} is the mass of *n*-butanol absorbed, ρ_{BuOH} and ρ_P are the densities of *n*-butanol and polymer, respectively [14].

Thermal properties were evaluated by differential scanning calorimetry (DSC: 2950, TA Instruments) at a heating rate of 10 °C min^{-1} from room temperature to 350 °C and thermogravimetric analysis (TGA: Q500 TA Instruments) at a heating rate of 10 °C min^{-1} from room temperature to 800 °C under N_2 atmosphere, respectively. From the DSC data, crystallinity of the samples was calculated according to the following formula.

$$Xc(\%) = \frac{\Delta H_m^{\mathrm{Sample}}}{\Delta H_m^*} \times 100$$

where *Xc* is crystallinity, $\Delta H_m^{\mathrm{Sample}}$ is the apparent enthalpy of fusion per gram of polymer sample which is obtained from the integral area of the base line and each melting curve in DSC, ΔH_m^* is the apparent enthalpy of fusion per gram of totally crystalline polymer. For PVdF, $\Delta H_m^* = 104.7$ J g^{-1} [14].

2.4. Electrochemical characterization

PGEs based on PVdF and PVdF/PEO membranes were prepared by activating a circular piece of as prepared electrospun membrane (area ~3 cm^2) with various liquid electrolytes. The capacity of the membrane to absorb liquid electrolyte i.e. electrolyte uptake (δ) was calculated using the relation:

$$\delta(\%) = \frac{M - M_0}{M_0} \times 100$$

where, M_0 is the mass of the dry membrane and M is the mass of the membrane after soaking in the electrolyte. The weight of the wet membrane was determined at different soaking intervals, after removing excess electrolyte on the surface by wiping softly with a tissue paper.

Ionic conductivity and interface phenomena were evaluated by impedance spectroscopy using Solartron 1470E and SI 1255B impedance/gain-phase analyzer coupled with a potentiostat, both interfaced with a personal computer. Measurements were carried out under open circuit conditions. A 20 mV AC perturbation was used and data were collected over a 10 mHz−1 MHz frequency range for both conductivity measurements and interface investigation. Ionic conductivity of the PGE is measured between −20 and 70 °C by sandwiching PGE between two stainless steel (SS) blocking electrodes using Swagelok® cells. All the cells are sealed in Ar-filled dry box and cells were placed in a temperature controlled environmental chamber. The cells were kept at each measuring temperature for 30 min to ensure thermal equilibration of the sample before measurement. Ionic conductivity (σ) was calculated as $\sigma = t/R_bA$; where t and A denote the thickness and area of the PGE, respectively and R_b is the bulk resistance obtained from the x-axis intercept of the complex AC impedance response with frequency. To study the interface phenomena, time dependant interfacial resistance (R_f) between lithium electrode and PGE was evaluated by monitoring the complex impedance response, on Li/PGE/Li symmetrical cells at room temperature over a period of 12 days of storage.

Two-electrode electrochemical coin cells were fabricated by placing the PGE between lithium metal anode (~300 μm thick) and carbon-coated lithium iron phosphate ($LiFePO_4$) cathode (~23 μm thick). The composite cathode was prepared by mixing 80 wt.% of active material, 10 wt.% of conducting additive (Super P Li carbon by Timcal) and 10 wt.% of PVdF binder (Sigma Aldrich) in *N*-methyl pyrrolidinone (NMP). The resulting slurry was coated onto aluminum foil (20 μm in thickness) using doctor blade technique and subsequently dried in the oven at 70 °C followed by pressing between stainless steel twin rollers and then punched into circular discs of 16 mm dia. Before the cell assembly, composite cathode was dried in a vacuum oven at 80 °C for 12 h to remove the residual solvent traces (if any). The test cells, Li/PGE/$LiFePO_4$ were fabricated in CR2016 coin cell and electrochemical tests were conducted using galvanostatic charge−discharge battery cycler (BTS XWJ, Neware Tech. Co.), between 2.5 and 4.0 V at room temperature at 0.1 C-rate. The activation of electrospun membrane to prepare PGE and the fabrication of test cells were carried out in an argon-filled glove box with oxygen and moisture level <0.1 ppm.

3. Results and discussion

3.1. Membrane morphology, porosity, electrolyte uptake and retention

Fig. 1 shows the surface morphology (FE-SEM images) of electrospun PVdF (Fig. 1a) and PVdF/PEO (Fig. 1b) membrane. The membranes consist of multilayered, three dimensional network structures of ultrafine fibers with bead free morphology. This indicates minimum axis symmetric instability of polymer fluid, rapid evaporation of the solvent during electrospinning and deposition of dry fibers on the collection drum. The interlaying of fibers provides enough mechanical strength for the easy handling of the fibrous membrane. The average fiber diameter (AFD) of the electrospun membrane was measured to be 1.5 and 1.9 μm for PVdF and PVdF/PEO membrane respectively. A number of parameters are known to influence the size and morphology of the fibrous membranes obtained by electrospinning. These include (i) material parameters such as molecular weight, molecular weight distribution of the polymers, (ii) solution parameters such as viscosity, surface tension and conductivity, (iii) process parameters such as applied voltage, flow rate, solution concentration, gap between the tip of the needle and collection target, and (iv) ambient parameters such as temperature, humidity and air velocity in the spinning chamber [15]. In the present study most of above parameters varied from a solution to another except solution concentration, flow rate, gap between tip of the needle to collection drum and ambient parameters. The difference in AFD and morphology of the membrane can be attributed to the difference in system parameters, solution parameters and applied voltage employed for the electrospinning. In the blend membrane, there is 10% PEO content, hence the viscosity and applied voltage greatly influence the AFD of the membrane. PVdF membrane was prepared at an applied voltage of 18 kV while PVdF/PEO membrane was prepared at 20 kV. The higher applied voltage ejects more fluid in a jet and thereby leads to larger fiber diameter. It is observed that PVdF fibers have a smooth surface finish (Fig. 1c), while PVdF/PEO fibers have a rough surface (Fig. 1d), which is beneficial for better adhesion with electrode and interfacial properties. The rough surface of the PVdF/PEO fibers may be due to the hygroscopic nature of PEO, which may absorb more moisture from the atmosphere during spinning and subsequent collection of fibers on the drum.

Porosity is one of the important factors that affects the amount of electrolyte absorbed by the electrospun membranes, which greatly influences the ionic conductivity and electrochemical properties of PGEs. The interlaying of the fibers generates porous structure in electrospun membrane. In electrospinning, solution viscosity plays a significant role on the porosity of the membranes. Low viscosity polymer solution makes thinner fluid jet at the tip of the needle resulting in the loose packing of fibers on the collection drum due to the rapid evaporation of the solvent, which leads to membranes with higher porosity. Porosity of the prepared membranes is determined by n-butanol uptake method. The n-butanol does not interact with the membrane; rather it penetrates the pores and occupies all the available pores, and thus gives a measure of the total pore volume of the membrane. The as prepared membrane has a porosity of ~80% with slightly higher value (~5%) for PVdF/PEO blend membrane. This difference may arise from the difference in membrane morphology, fiber diameter, tortuosity and uniformity of pore distribution in the membranes which is strongly dependent on the spinning parameters and solution properties [15]. The membranes prepared here showed higher porosity compared to that reported for electrospun PVdF (<80%) [16] and P(VdF-*co*-HFP) membrane (<75%) by Kim et al. [17] with membranes of AFD 1.3 μm. The difference in porosity might be due to the variations in solution properties and experimental parameters adopted for electrospinning in different studies. It is inferred that fibrous membrane in the present study contains loosely packed fibers, which leads to higher porosity.

Electrolyte uptake of the membrane in different electrolyte solutions was determined over a period of 1 h. The electrolyte uptake varies from 590% for 1 M $LiCF_3SO_3$ to 750% for 1 M LiTFSI in EC/DEC. The order of uptake of PVdF/PEO membrane with different

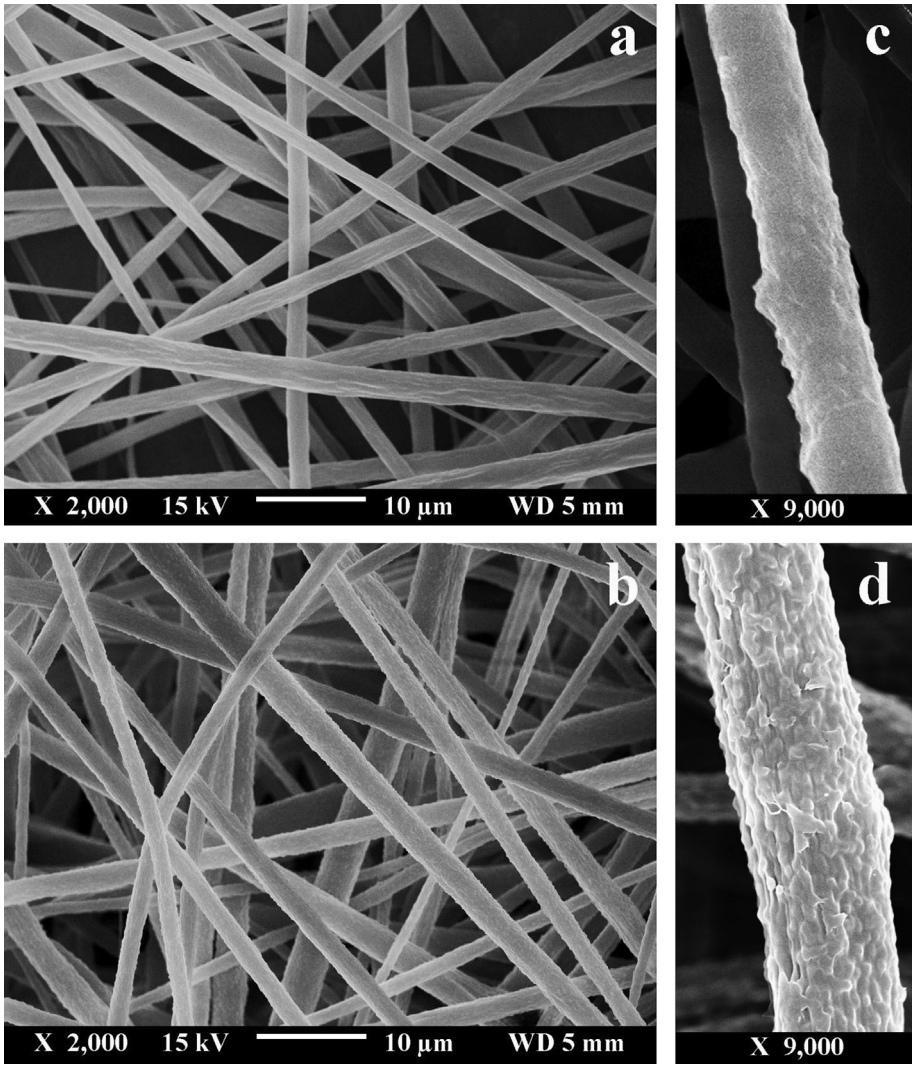

Fig. 1. FE-SEM image of electrospun membrane; (a) PVdF, (b) PVdF/PEO blend; magnified image of fiber; (c) PVdF, (d) PVdF/PEO polymer blend fiber.

electrolyte is as follows; LiTFSI (750) > $LiPF_6$ (690) >$LiClO_4$ (675) > $LiBF_4$ (630) > $LiCF_3SO_3$ (590). The difference in uptake of different electrolytes is attributed to varying viscosity of the electrolyte mixture and also the interaction and affinity of the lithium salt to the polymeric matrix [18,19]. The electrolyte uptake of the porous membrane is also greatly dependent on the porosity and pore structure of the membrane. The uptake of PVdF membrane with 1 M $LiPF_6$ is found to be 650%, which is lower than PVdF/PEO membrane with same electrolyte. The higher porosity and presence of PEO leads to the higher uptake for the blend membrane. It was observed that uptake process is rapid and gets stabilized within 15 min which can be attributed to the high porosity, fully interconnected pores and interlaid fiber structure of the membranes and good affinity to the electrolytes solution. The electrospun membrane displays sufficient mechanical strength and easy handling even after activation with the various electrolytes.

3.2. Thermal characterization

The effect of blending low melting point PEO with PVdF on the thermal stability of the electrospun membrane is studied using TGA and DSC. Fig. 2 shows the TGA plot of both the polymers and blended electrospun membrane. As seen in Fig. 2, PVdF/PEO membrane showed intermediate thermal stability compared to the

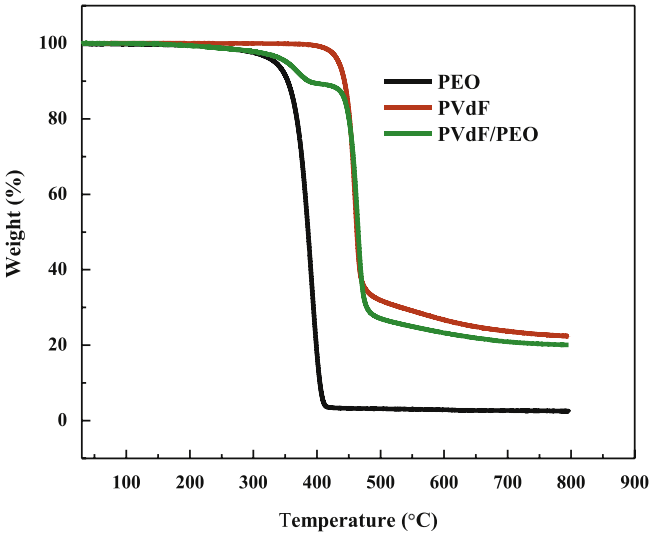

Fig. 2. TGA curves of pristine PVdF (powder), PEO (powder) and PVdF/PEO blend polymer film (electrospun membrane) under N_2 atmosphere at a heating rate of 10 °C min^{-1}.

component polymers. It is seen that TGA curve of PVdF/PEO membrane shows a characteristic two step weight loss, with the first short peak at a temperature 347 °C and longer peak at 433 °C corresponding to the decomposition temperature of PEO and PVdF respectively. It can be seen that first decomposition peak of the electrospun membrane is slightly shifted to higher temperature from that of pristine PEO (318 °C) and PVdF (419 °C). This can be attributed to interaction between PEO and PVdF in the polymer blend which leads to good mechanical and thermal stability. At a temperature of 412 °C, pristine PEO is completely decomposed. At 800 °C, a char yield of 21% is observed for PVdF/PEO membrane, which is about 85% char yield of pristine PVdF, proving that prepared electrospun membrane has good thermal stability.

Fig. 3 shows the DSC curves of the polymers and PVdF/PEO electrospun membrane. Similar to the TGA curve, DSC curve also shows the characteristic peaks of both PVdF and PEO. The melting endotherm at 65 and 157 °C corresponds to PEO and PVdF respectively. PEO exhibits a crystalline melting transition, starting at 50 °C, with a melting peak (T_m) at 65 °C. The polymer is predominantly crystalline since a well-defined glass transition (T_g) corresponding to the amorphous phase is absent. PVdF/PEO blend membrane has two T_m at 61 and 156 °C, corresponding to the melting temperatures of PEO and PVdF. This implies during spinning the polymers are phase separated. There is only one melting temperature observed for the film prepared by solution casting. This indicates that homogeneous blending of PVdF and PEO has been accomplished as a result of the possible chemical-oriented coordination between the 'mer' units of the above two polymers which assures better blending. This implies the microphase separation is accomplished in the syringe because of keeping the solution without stirring for long time while spinning [20]. The lower T_m of PEO in the blend when compared with pristine PEO implies the existence of interactions between ether "O" atoms of PEO and F atoms in the PVdF that lead to an inhibition of the effective reorganization of PEO chains for crystallization to occur [21]. The endotherm corresponding to PEO is very shallow when compared to pristine PEO proving that crystallinity has been marginally reduced by blending with PVdF. It is observed that the heat of fusion for the blend membrane is slightly higher than pristine PVdF powder, which indicates higher crystallinity. The crystallinity of PVdF and PVdF/PEO membrane is shown to be 40.5 and 42.3% respectively. The higher crystallinity of the electrospun membrane probably results from the orientation of the polymer to the fiber axis when it drawn to form nanofibers.

3.3. Ionic conductivity

Ionic conductivity of membranes activated with different electrolytes was measured by AC impedance in the temperature range −20 and 70 °C. Fig. 4 shows the AC impedance spectra of electrospun PVdF/PEO blend electrolytes in SS/PGE/SS cell at 30 °C. The impedance responses are typical of the electrolytes where the bulk resistance (R_b) is the major contribution to the total resistance and only a minor contribution comes from grain boundary resistance. It is observed that impedance response of PGEs at a temperature between −20 and 70 °C (the minimum and maximum temperatures studied here) is in the form of a straight line inclined about 45° with respect to the real axis from high to lower frequencies. This type of behavior is typical for a PGE sandwiched between two quasi-blocking electrodes [15]. At 30 °C, the intercept on the real-axis representing R_b of the electrolyte varies between 1.5 and 4.5 Ω. At 70 °C, it is observed that ionic resistance of PVdF/PEO decreases considerably with a shift of the inclined spike to higher frequency. Such a behavior is observed at temperatures above 60 °C, where the crystalline segments of PEO melt, increasing the overall mobility of ions in the electrolyte. Compared to $LiCF_3SO_3$, the ionic resistance of PGE activated with LiTFSI is seen to be very low even at the lower temperature of 25 °C. This implies that incorporation of LiTFSI significantly reduces the electrolyte resistance due to its lower viscosity, and enhances the mobility of Li^+ ions in the electrolyte.

The variation of ionic conductivity with temperature from −20–70 °C is presented in Fig. 5. Ionic conductivity of the PGEs at 30 °C (mS cm^{-1}) follows the order LiTFSI (4.9) > $LiPF_6$ (4.5) > $LiClO_4$ (4.2) > $LiBF_4$ (2.8) > $LiCF_3SO_3$ (1.8). The results indicate that electrospun membrane based PGE can function well by providing easy transport of ions between the electrodes in lithium-ion cells. The ionic conductivity follows the same trend as the electrolyte uptake (Table 1). There are several contrasting factors that affect the ionic conductivity of the electrolyte solutions. Two opposing factors that affect the ionic conductivity are the average ion mobility and dissociation constant of the lithium salts in solution. In general higher the

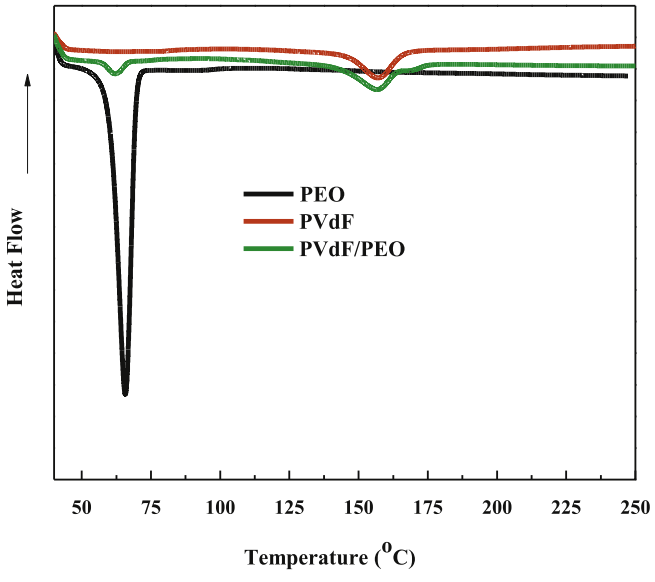

Fig. 3. DSC thermograms of pristine PVdF, PEO and PVdF/PEO blend polymer film (electrospun membrane) at a heating rate of 10 °C min^{-1}.

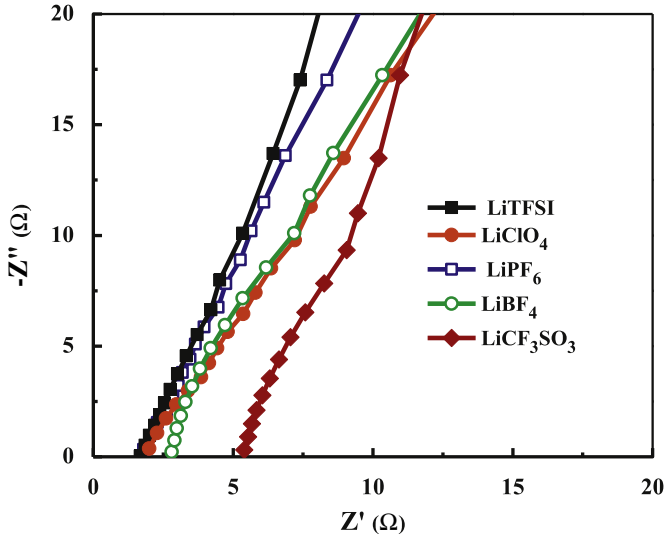

Fig. 4. AC impedance spectra of polymer electrolytes based on electrospun PVdF/PEO blend membranes activated with different electrolytes at 30 °C, (SS/PGE/SS cells, frequency range 10 mHz–1 MHz, amplitude 20 mV).

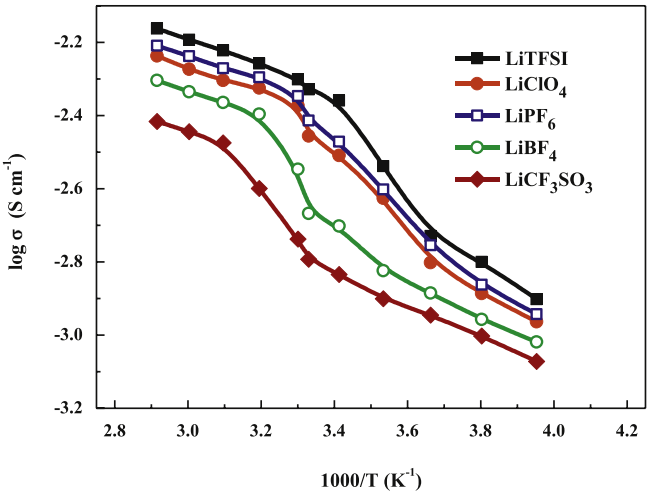

Fig. 5. Effect of temperature on ionic conductivity of polymer electrolytes based on electrospun PVdF/PEO polymer blend membranes activated with different electrolytes (SS/PGE/SS cells frequency, 10 mHz–1 MHz, amplitude 20 mV).

dissociation constant and greater the average ion mobility, higher is the ionic conductivity, when the solvent system is constant. The average ion mobility follows the order $LiBF_4 > LiClO_4 > LiPF_6 > LiCF_3SO_3 >$ LiTFSI and the dissociation constant follows the order $LiCF_3SO_3 < LiBF_4 < LiClO_4 < LiPF_6 <$ LiTFSI [13]. Among the electrolytes studied here, LiTFSI has the highest dissociation constant and $LiBF_4$ has the highest ion mobility. The ionic conductivity of the PGE is dependent on number of charge carriers as per the equation $\sigma = \Sigma N_i R_i \dot{E}_i$, where N_i, R_i and $\dot{E}_i$ are number of charge carriers, ionic charge and ionic mobility, respectively. Here the electrolyte uptake of LiTFSI is highest and also it has the highest dissociation constant, therefore there will be greater number of free charge carriers leading to higher ionic conductivity. It is seen that the dissociation constant of the liquid electrolyte affects the ionic conductivity more significantly than the average ion mobility. The ionic conductivity of PVdF/PEO blend membrane activated with 1 M LiTFSI in EC/DEC varies between 4.0×10^{-3} S cm^{-1} at 20 °C and 6.9×10^{-3} S cm^{-1} at 70 °C. The change in slope of the curve at room temperature is typical of PGEs and has been attributed to the change in conduction mechanism of the electrolyte. The sharp decrease in conductivity below 10 °C is due to the freezing property of carbonate solvents in the electrolyte solution. At a temperature of 35 °C, the conductivity of PVdF and PVdF/PEO membrane activated with 1 M $LiPF_6$ in EC/DEC is 3.2×10^{-3} and 5.3×10^{-3} S cm^{-1}, respectively, while the ionic conductivity of Celgard (2320) in the same electrolyte is observed to be 2.1×10^{-5} S cm^{-1}. Compared to PVdF membrane, the higher conductivity of PVdF/PEO is associated with the PEO crystalline-amorphous phase transition, which enhances the ion mobility and segmental motion of the polymer chains. Hence the Li^+ ions coordinated with the 'O' atoms of PEO segments could be freed partially or fully which could lead to larger number of charge carriers with improved charge migration. It is observed that polymer blend containing higher PEO content (30%) has higher ionic conductivity [20]. Hence it is clear that addition of PEO showed a pronounced effect on ionic conductivity of PGEs based on electrospun PVdF membrane. Higher ionic conductivity is also reported for PVdF/PEO [20] and PEO/polystyrene [22] blend solid polymer electrolytes with increasing PEO content.

Table 1
Electrolyte uptake and ionic conductivity of PGEs activated with different electrolytes (electrolyte: 1 M solution of lithium salt in1:1 w/w EC/DEC).

Membrane	Electrolyte[a]	Uptake (%)	Ionic conductivity (S cm^{-1}) at 30 °C
PVdF/PEO	LiTFSI	750	4.9
	$LiPF_6$	690	4.5
	$LiClO_4$	675	4.2
	$LiBF_4$	630	2.8
	$LiCF_3SO_3$	590	1.8
			Ionic conductivity (S cm^{-1}) at 35 °C
PVdF	$LiPF_6$	650	3.2
PVdF/PEO	$LiPF_6$	690	5.3
Celgard (2320)	$LiPF_6$	200	2.1×10^{-2}

[a] 1 M solution of lithium salts in EC/DEC (1:1 w/w).

Fig. 5 depicts the Arrhenius plots of logarithmic conductivity versus inverse temperature for PVdF/PEO polymer electrolytes activated with different lithium salts. Effectively, it is noticed from Fig. 5, the curve shows three linear regions (Arrhenius behavior) with change in slope indicating the three different activation energies involved for the ion transport as function of temperature. The three slops observed between −20 and 25, 25 to 40 and 40–70 °C. The transition temperature (25 and 40 °C) found by intercepting the two linear portions, corresponds to the freezing point of carbonate solvents in the electrolyte and melting of crystalline phase of PEO respectively. The decrease in activation energy together with significant rise in conductivity (at or above 40 °C) is presumably due to the softening and melting of crystalline phase of PEO near 60 °C making the polymer electrolyte fully amorphous and hence the conductivity enhancement. Obviously, this amorphous structure facilitates the fast lithium ion motion in the polymer network and it further provides higher free volume in the polymer electrolyte system upon increasing the temperature. It is seen that log σ versus 1/T curves for all the PGEs are slightly curved, so the activation energy for ionic conduction E_a can be obtained using the Vogel-Tamman–Fulcher (VTF) model $\{\sigma = \sigma_0 T^{-1/2} \exp[(-E_a/R(T - T_0)]\}$ instead of the simple Arrhenius model ($\sigma = \sigma_0 \exp(-E_a/RT)$ used for the treatment of the linear plots. This indicates that the conduction mechanism not only involves the increasing dissociation of lithium salt but also the segmental motion of the polymer chains. In the present study the high ionic conductivity achieved can be attributed to the combination of two approaches. The addition of PEO to PVdF to form a uniform blend improves the segmental motion of the electrospun polymeric host. PEO owing to its structure offers excellent segmental motion of the polymeric chains, while PVdF acts as the inert host that provides mechanical strength to the PGE. PEO is soluble in the liquid electrolyte [2], therefore PVdF acts as the mechanical substrate, but PVdF by itself had good affinity to the electrolytes, which help in achieving high values of electrolyte uptake. Thus the beneficial properties of both the host polymers are utilized to form a blended polymeric host with high ionic conductivity.

3.4. Electrochemical properties evaluation

3.4.1. Interfacial resistance

Fig. 6 illustrates the initial complex impedance response of Li/PGE/Li symmetric cells and their impedance after 12 days storage measured at open circuit potential at ambient temperature. Interfacial stability of PGE with lithium metal electrode is an essential factor to demonstrate their performance in LIBs. Impedance spectrum shows a distorted semi circle in the middle frequency range, and its expansion with storage time indicates the formation and growth of passivation layer at the PGE and lithium metal electrode interface. The growth of passivation layer is associated with the decomposition of the electrolyte or the reaction between the electrolyte and the Li-metal electrode [1,12,13]. The nature of the lithium salt significantly affects the reaction of the electrolyte with the electrode and thereby affects the interfacial resistance [13]. The

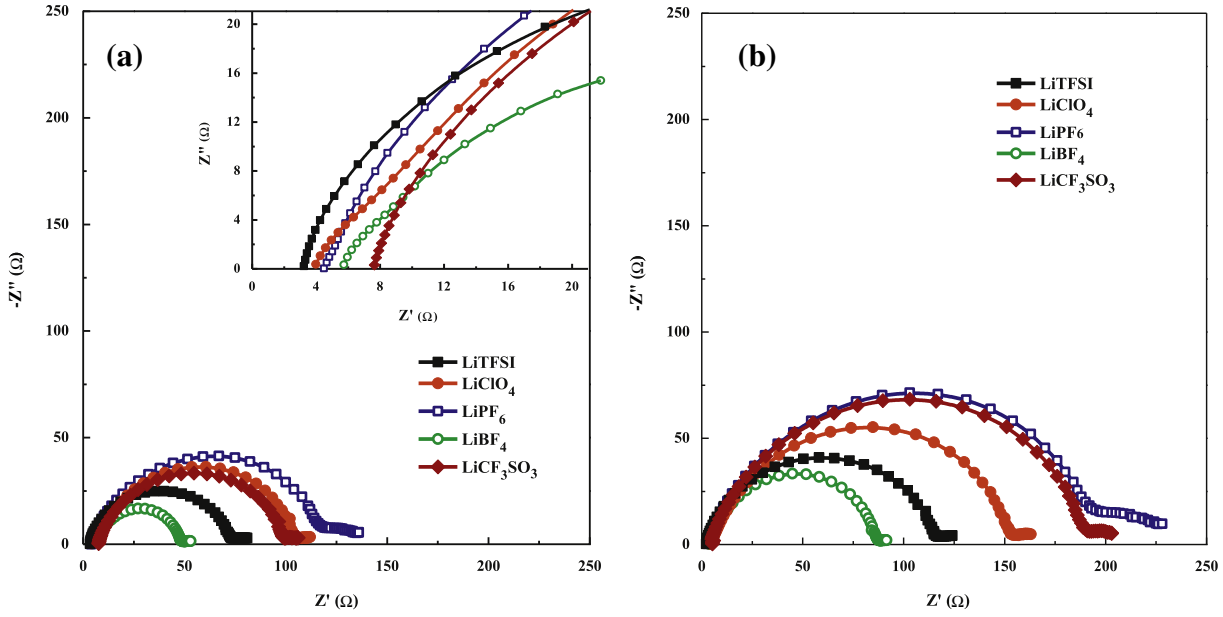

Fig. 6. AC impedance behaviors of polymer electrolytes based on electrospun PVdF/PEO polymer blend membranes (Li/PGE/Li cells, frequency range 10 mHz–1 MHz, amplitude 20 mV): (a) initial impedance and (b) impedance after 12 days of storage.

initial interfacial resistance (R_i) of PGE follows the order $LiBF_4$ (48.7) < LiTFSI (73) < $LiCF_3SO_3$ (99.8) < $LiClO_4$ (106) < $LiPF_6$ (122 Ω).

As shown in the magnified region of Fig. 6a, low bulk resistance (R_b) of PGEs is observed to be in well-agreement with that observed for SS/PGE/SS symmetric cells (discussed earlier in Sec. 3.3). Fig. 7 shows the change in interfacial resistance as a function of storage time. It is observed that there is no significant increase in R_b with storage time and membranes are able to retain their high ionic conductivity and dimensional stability. As shown in Fig. 7, R_f for all PGEs increased with storage time, but the increase is very low as compared to other PGEs based on electrospun PVdF [16] or P(VdF-*co*-HFP) [5] or PVdF based phase inversion membranes [23]. The increase in R_f with storage time may be associated with the growth of passivation layer on the lithium electrode surface and degradation of physical contact between the electrode and PGE. After one day of storage all the PGEs show significant increase in R_f, which is about 100–135% higher than R_i. The R_f of all the PGEs gets stabilized within 9 days indicating good stability with lithium metal. After a period of storage of 12 days the R_f values (Ω) follows the order $LiBF_4$ (85) < LiTFSI (115) < $LiClO_4$ (149) <$LiCF_3SO_3$ (186) < $LiPF_6$ (215), which is about 150–170% higher than R_i. This low increment in R_f for all the PGEs shows their good electrochemical stability and compatibility with lithium metal anode.

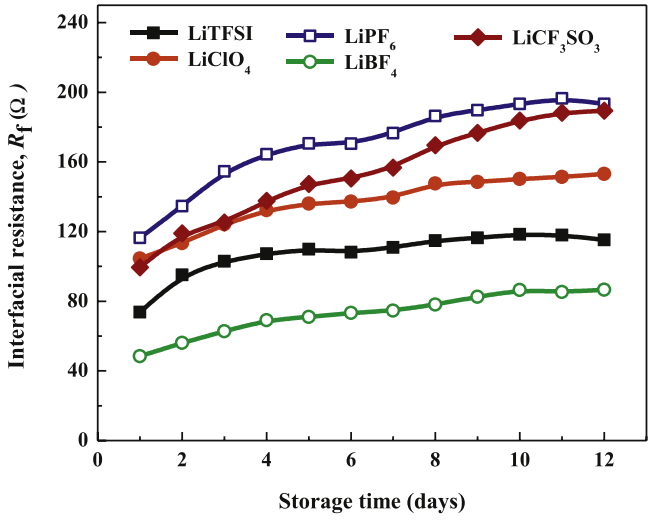

Fig. 7. Time dependant interfacial behaviors for PGE based on electrospun PVdF/PEO polymer blend membrane with different electrolytes (Li/PGE/Li cell, frequency range 10 mHz to 1 MHz).

3.4.2. *Evaluation in Li/LiFePO4 cell*

Compared with conventional cathode materials based on transition metal oxides widely used in LIBs, $LiFePO_4$ has been chosen because it is environmentally benign, thermally stable, non-toxic, cheap and easy to fabricate. $LiFePO_4$ has higher theoretical capacity (170 mAh g^{-1}), flat operating voltage of 3.4 V and excellent cycling properties at low C-rate. Li/PGE/$LiFePO_4$ cells were assembled and cycled at 0.1 C rate between 2.5 and 4 V at room temperature. The cells with PGE based on electrospun membrane activated with LiTFSI and $LiClO_4$ are wisely selected for the cell studies due to their high ionic conductivity and better compatibility with lithium metal. The first cycle charge–discharge properties at a current density corresponding to 0.1 C-rate are compared in Fig. 8. The cell with PVdF/PEO blend PGE based on LiTFSI shows an initial discharge capacity of 168 mAh g^{-1}, while the cell with PGE comprising $LiClO_4$ shows 165 mAh g^{-1}, which corresponds to ~98 ± 1% utilization of the active material. The discharge capacity of the cell assembled with blend polymer electrolyte is higher compared to the cell with electrospun PVdF membranes. The cell with PGE based on electrospun PVdF activated with LiTFSI and $LiClO_4$ showed a discharge capacity of 148 mAh g^{-1}, which is about 11% less than the cell with PGE based on PVdF/PEO polymer blend membrane. The difference in capacity may due to the difference in ionic conductivity of PGE discussed in Sec. 3.3. It was reported that the discharge capacity of the cell assembled with $LiFePO_4$/Li-metal using PGE based on electrospun P(VdF-*co*-HFP) activated with 1 M $LiPF_6$ is about 140 mAh g^{-1} [14,18].

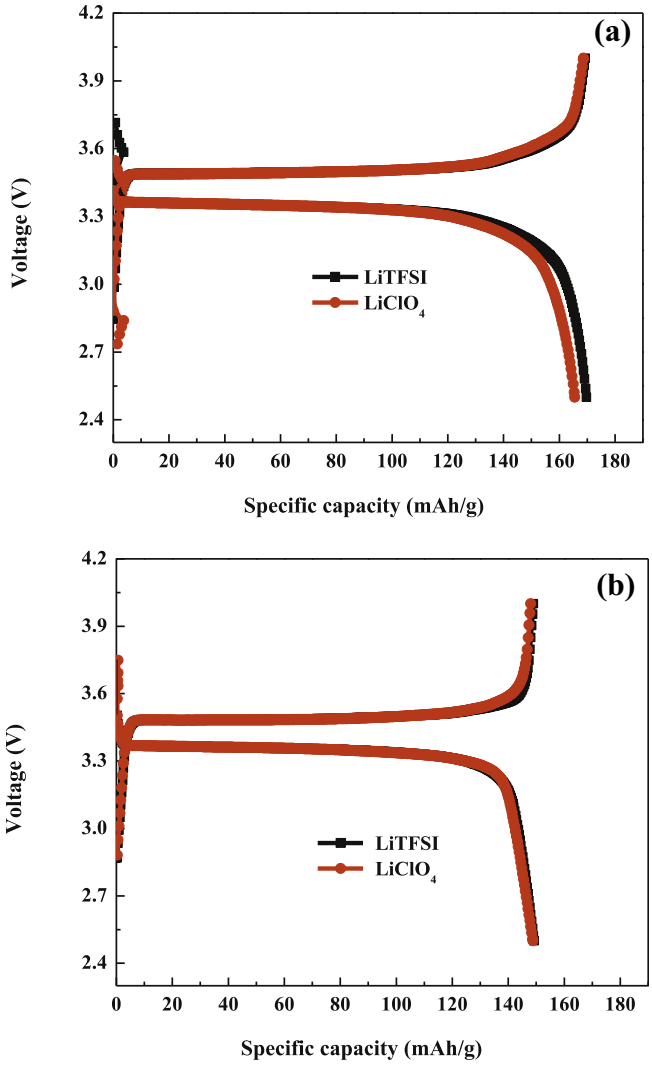

Fig. 8. Initial charge–discharge properties of Li/PGE/$LiFePO_4$ cells with polymer electrolytes based on electrospun membranes (25 °C, 0.1 C rate, 2.5–4.0 V): (a) PVdF/PEO polymer blend and (b) PVdF.

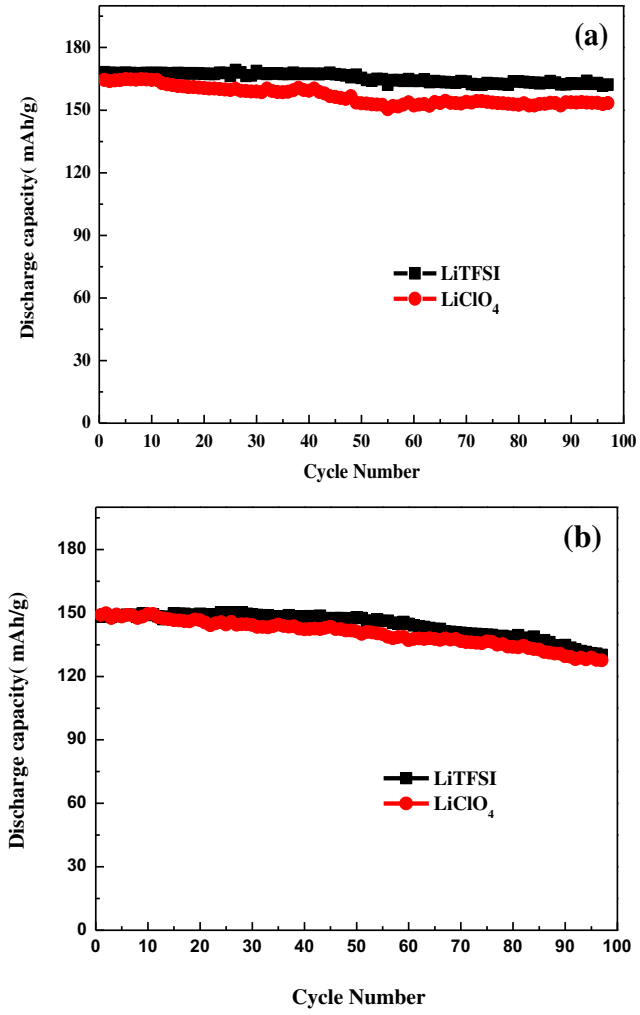

Fig. 9. Cycling properties of Li/PGE/$LiFePO_4$ cells with polymer electrolyte based on electrospun membrane (25 °C, 0.1 C rate, 2.5–4.0 V): (a) PVdF/PEO polymer blend and (b) PVdF.

The cycling performance of the Li/$LiFePO_4$ cells with LiTFSI and $LiClO_4$ based PGEs are shown in Fig. 9. It is observed that all the cells show relatively stable performance without significant capacity fading. After 50 cycles, the cells with PVdF/PEO polymer blend membranes (Fig. 9a) delivers a discharge capacity of 162 and 152 mAh g^{-1}, respectively for LiTFSI and $LiClO_4$. As shown in Fig. 9b, it was observed that, after 50 cycles, the cell comprised of PVdF membrane activated with LiTFSI and $LiClO_4$ delivers a discharge capacity of ~128 mAh g^{-1}. The observed capacity fade may be due to the progressive decomposition and/or leakage of the electrolyte. Also the structural characteristics and composition of cathode materials play a vital role on the capacity of the cell and cycling performance. The capacity retention ratio of the cell with PVdF/PEO polymer blend membrane activated with LiTFSI electrolyte is 95% and $LiClO_4$ is 89% (calculated based on initial discharge capacity), while the cell with PVdF membrane shows only ~86% retention. The relatively stable performance with good capacity retention proves that PEO have significant effect on the ionic conductivity and electrochemical properties of PGEs based on electrospun PVdF. The study also demonstrated suitability of the PGEs based on PVdF/PEO polymer blend electrospun membrane for application in LIBs.

4. Conclusions

Electrospun fibrous membranes of PVdF and PVdF/PEO are prepared. The spinning parameters are controlled to get a bead-free membrane with high porosity, uniform fiber distribution and sufficient mechanical strength. The membranes have inter-connected fibrous morphology with voids/pores. The suitability of the membrane as host matrix for the preparation of polymer gel electrolyte for lithium-ion battery application is explored. PVdF/PEO fibrous membranes exhibit a high uptake of liquid electrolyte (lithium salt in EC/DEC) and transform into polymer gel electrolyte. The PVdF/PEO membranes exhibits high ionic conductivity at room temperature, better than that of Celgard and PE based on electrospun PVdF membrane. The polymer gel electrolyte performs with stable charge–discharge characteristics when evaluated as separator-cum-electrolyte in a lithium-ion cell. The performance characteristics of PVdF/PEO membranes as polymer electrolytes in lithium batteries are much superior to PVdF membrane. Thus, the present methodology for preparing polymer electrolytes using electrospinning can be extended for the preparation of wide range of other polymer composites membranes.

References

[1] S. Ahmad, Ionics 15 (2009) 309–321.
[2] B. Scrosati, C.A. Vincent, MRS Bull. (2000) 28–30.
[3] P. Raghavan, X. Zhao, J. Manuel, C. Shin, M.Y. Heo, J.H. Ahn, H.S. Ryu, H.J. Ahn, J.P. Noh, G.B. Cho, Mater. Res. Bull. 45 (2010) 362–366.
[4] P. Raghavan, J.W. Choi, J.H. Ahn, G. Cheruvally, G.S. Chauhan, H.J. Ahn, C. Nah, J. Power Sources 184 (2008) 437–443.
[5] P. Raghavan, X. Zhao, J. Manuel, G.S. Chauhan, J.H. Ahn, H.S. Ryu, H.J. Ahn, K.W. Kim, C. Nah, Electrochim. Acta 55 (2010) 1347–1354.
[6] G. Appetecchi, F. Croce, J. Hassoun, B. Scrosati, M. Salomon, F. Cassel, J. Power Sources 114 (2003) 105–112.
[7] J.H. Shin, Y.T. Lim, K.W. Kim, H.J. Ahn, J.H. Ahn, J. Power Sources 107 (2002) 103–109.
[8] J. Le Nest, A. Gandini, H. Cheradame, Br. Polym. J. 20 (1988) 253–268.
[9] A. Du Pasquier, P.C. Warren, D. Culver, A.S. Gozdz, G.G. Amatucci, J.M. Tarascon, Solid State Ionics 135 (2000) 249–257.
[10] Z.H. Li, Q.Z. Xiao, P. Zhang, H.P. Zhang, Y.P. Wu, T. Van Ree, Funct. Mater. Lett. 01 (2008) 139.
[11] R. Prasanth, V. Aravindan, M. Srinivasan, J. Power Sources 202 (2012) 299–307.
[12] F.B. Dias, L. Plomp, J.B.J. Veldhuis, J. Power Sources 88 (2000) 169–191.
[13] K. Xu, Chem. Rev. 104 (2004) 4303–4417.
[14] P. Raghavan, X. Zhao, J. Kim, J. Manuel, G. Chauhan, J. Ahn, C. Nah, Electrochim. Acta 54 (2008) 228–234.
[15] P. Raghavan, J. Manuel, X. Zhao, D.S. Kim, J.H. Ahn, C. Nah, J. Power Sources 196 (2011) 6742–6749.
[16] J.R. Kim, S.W. Choi, S.M. Jo, W.S. Lee, B.C. Kim, Electrochim. Acta 50 (2004) 69–75.
[17] J.R. Kim, S.W. Choi, S.M. Jo, W.S. Lee, B.C. Kim, J. Electrochem. Soc. 152 (2005) A295.
[18] X. Li, G. Cheruvally, J. Kim, J. Choi, J.H. Ahn, K. Kim, H.J. Ahn, J. Power Sources 167 (2007) 491–498.
[19] J.W. Choi, J.H. Kim, G. Cheruvally, J.H. Ahn, K.W. Kim, H.J. Ahn, J.U. Kim, J. Ind. Eng. Chem. 12 (2006) 939–949.
[20] M. Jacob, S. Prabaharan, S. Radhakrishna, Solid State Ionics 104 (1997) 267–276.
[21] J.W. Choi, G. Cheruvally, Y.H. Kim, J.K. Kim, J. Manuel, P. Raghavan, J.H. Ahn, K.W. Kim, H.J. Ahn, D.S. Choi, C.E. Song, Solid State Ionics 178 (2007) 1235–1241.
[22] F.M. Gray, J.R. MacCallum, C.A. Vincent, Solid State Ionics 18 (1986) 282–286.
[23] X. He, Q. Shi, X. Zhou, C. Wan, C. Jiang, Electrochim. Acta 51 (2005) 1069–1075.